Contribution from the Departments of Chemistry, University of Vermont, Burlington, Vermont 05405, Worcester Polytechnic Institute, Worcester, Massachusetts 01609, and University of Michigan, Ann Arbor, Michigan 48104, and Contribution No. 2754 from the Central Research and Development Department, Experimental Station, E. I. du Pont de Nemours and Company, Wilmington, Delaware 19898

Stereodynamics of the Ligand-Metal Bond. Phosphorus-31 DNMR Studies of Internal Rotation about Rhodium-Phosphorus Bonds in *trans*-[RhX(CO)L_2] Complexes (X = Halogen; L = Tertiary Phosphine)

C. HACKETT BUSHWELLER,*[1a] STEVEN HOOGASIAN,[1b] ALAN D. ENGLISH,[1c] J. STANLEY MILLER,[1d] and MARILYN Z. LOURANDOS[1b]

Received December 17, 1980

The $^{31}P\{^1H\}$ DNMR spectra of a series of rhodium(I) square-planar (d^8) complexes of the type *trans*-[RhX(CO)L_2] in which L = $(t\text{-}C_4H_9)_2PCH_3$, $(t\text{-}C_4H_9)_2PCl$, or $(t\text{-}C_4H_9)_2P(C_6H_5)$ and X = Cl, Br, or I show changes consistent with slowing intramolecular conformational exchange. The $^{31}P\{^1H\}$ NMR spectrum of each complex at slow exchange can be interpreted in terms of different conformers. DNMR line-shape analyses of the exchange-broadened spectra speak for a specific stepwise interconversion among the various conformers rather than a nonselective exchange pathway. Such a stepwise itinerary is consistent with simple internal rotation about the rhodium-phosphorus bonds.

Previous research in our laboratory has shed some light on the intramolecular stereodynamics of tertiary phosphines[2] and bis(phosphines).[3] In addition, we have examined the effects of complexation on carbon-phosphorus bond rotation in tertiary phosphine boranes[4] and $LM(CO)_5$ complexes (L = tertiary phosphine; M = Cr, Mo, W).[5] This work led us to examine the dynamic stereochemistry of a series of *trans*-bis(phosphine)halocarbonylrhodium(I) systems.

Planar four-coordinate Rh(I) complexes play key roles in catalysis of the hydroformylation reaction (e.g., Rh[P-$(C_6H_5)_3]_2$(CO)Cl) and the homogeneous hydrogenation of alkenes and acetylenes (e.g., Rh[$P(C_6H_5)_3]_3$Cl).[6] Solution conformational preferences and conformational exchange rates may be factors in determining the stereospecificity of asymmetric induction by related complexes.[7] Many studies of rhodium complexes using techniques such as electronic spectroscopy,[8] ^1H and ^{31}P nuclear magnetic resonance spectroscopy,[9] infrared spectroscopy,[9] and X-ray diffraction[10] have shed light on the gross structure and the nature of metal-ligand bonding in these systems. There have been reports concerning "dynamic" NMR (DNMR) studies of ligand exchange and restricted internal rotation for complexes of various metals including Rh(I).[11,12] However, for metal-phosphine complexes, there is generally a dearth of information regarding the roles of steric and/or electronic factors in determining conformational preferences in solution and rates of internal rotation about metal-phosphine bonds. This paper concerns some detailed $^{31}P\{^1H\}$ DNMR studies of restricted rotation about Rh-P bonds for a series of Rh(I) complexes.

Results and Discussion

***trans*-Rh[$(t\text{-}C_4H_9)_2PCH_3]_2$(CO)Cl (1).** Examination of the 36.43-MHz $^{31}P\{^1H\}$ DNMR spectrum of **1** (0.18 M in 50:50

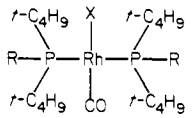

1: R = CH_3; X = Cl
2: R = X = Cl
3: R = Cl; X = Br
4: R = Cl; X = I
5: R = C_6H_5; X = Cl

CD_2Cl_2/toluene, v/v) at 65 °C shows a broadened doublet centered at δ 42.92 (downfield relative to external 85% H_3PO_4). The doublet is due to spin-spin coupling of ^{31}P to ^{103}Rh ($I = {}^1/_2$; 100% natural abundance). The value of $^1J_{RhP}$ at 65 °C is approximately 120 Hz. The spectrum of **1** at 65 °C is consistent with both phosphorus atoms being magnetically equivalent *or* with rapid equilibration of the phosphorus atoms among different environments. As shown in the spectra of **1** at lower temperatures (Figure 1), it is the latter interpretation which is correct.

It should be noted at this point that the observation of Rh-P spin-spin coupling at 65 °C (Figure 1) indicates that *phosphine ligand dissociation (i.e, Rh-P bond breaking) is slow on the ^{31}P DNMR time scale.* Thus, it may be safely assumed that dissociation of the phosphine ligands does not occur at any significant rate at temperatures below 65 °C and any changes in the spectra must be due to some other process.

At temperatures below 65 °C, the spectrum of **1** broadens asymmetrically and is separated at -73 °C into a series of well-resolved signals (Figure 1). A complete line-shape simulation of the spectrum at -73 °C using a locally modified version of computer program DNMR3[13] reveals that the spectrum consists of the B_2 doublet of a B_2X spin system (X = ^{103}Rh) centered at δ 44.94 ($^1J_{RhP}$ = 118.0 Hz; population relative to area of total spectrum 0.73), the D_2 doublet of a D_2X spin system at δ 28.97 ($^1J_{RhP}$ = 120.0 Hz; relative pop-

(1) (a) University of Vermont; Alfred P. Sloan Research Fellow; Camille and Henry Dreyfus Teacher-Scholar. (b) Worcester Polytechnic Institute. (c) E. I. du Pont de Nemours and Co. (d) University of Michigan.
(2) Bushweller, C. H.; Brunelle, J. A. *J. Am. Chem. Soc.* **1973**, *95*, 5949.
(3) Brunelle, J. A.; Bushweller, C. H.; English, A. D. *J. Phys. Chem.* **1976**, *80*, 2598.
(4) Bushweller, C. H.; Brunelle, J. A. *Tetrahedron Lett.* **1974**, *893*.
(5) Bushweller, C. H.; Lourandos, M. Z. *Inorg. Chem.* **1974**, *13*, 2514.
(6) (a) Livingstone, S. E. *Compr. Inorg. Chem.* **1973**, *3*, 1237. (b) Osborn, J. A.; Jardine, F. H.; Young, F. H.; Wilkinson, G. *J. Chem. Soc. A* **1966**, 1711.
(7) Tolman, C. A. *Chem. Rev.* **1977**, *77*, 313.
(8) Brady, R.; Flynn, B. R.; Geoffroy, G. L.; Gray, H. B.; Peone, J.; Vaska, L. *Inorg. Chem.* **1976**, *15*, 1485.
(9) (a) Brown, T. H.; Green, P. J. *J. Am. Chem. Soc.* **1970**, *92*, 2359. (b) Brown, T. H.; Green, P. J. *Ibid.* **1969**, *91* 3378. (c) Mann, B. E.; Shaw, B. L.; Slade, R. M. *J. Chem. Soc. A* **1971**, 2976. (d) Tolman, C. A.; Meakin, P. A.; Lindner, D. L.; Jesson, J. P. *J. Am. Chem. Soc.* **1974**, *96*, 2762.
(10) (a) Wei, C. H.; Wilks, G. R.; Dahl, L. F. *J. Am. Chem. Soc.* **1967**, *89*, 4792. (b) Corey, E. R.; Dahl, L. F.; Beck, W. *Ibid.* **1963**, *85*, 1202.
(11) English, A. D.; Meakin, P.; Jesson, J. P. *J. Am. Chem. Soc.* **1976**, *98*, 7590 and references therein.
(12) (a) Empsall, H. D.; Hyde, E. M.; Mentzer, E.; Shaw, B. L. *J. Chem. Soc. Dalton Trans.* **1977**, 2285. (b) Empsall, H. D.; Mentzer, E.; Pawson, D.; Shaw, B. L., Mason, R.; Williams, G. A. *J. Chem. Soc., Chem. Commun.* 1977, 311. (c) Mann, B. E.; Masters, C.; Shaw, B. L.; Stainbank, R. E. *Ibid.* **1971**, 1103. (d) Bright, A.; Mann, B. E.; Masters, C.; Shaw, B. L.; Slade, R. M.; Stainbank, R. E. *J. Chem. Soc. A* **1971**, 1826.

(13) The original version of the computer program DNMR3 was written by: Kleier, D. A.; Binsch, G. *J. Magn. Reson.* **1970**, *3*, 146. Our modifications are described in: Bushweller, C. H.; Bhat, G.; Letendre, L. J.; Brunelle, J. A.; Bilofsky, H. S. Ruben, H.; Templeton, D. H.; Zalkin, A. J. *J. Am. Chem. Soc.* **1975**, *97*, 65.

0020-1669/81/1320-3448$01.25/0

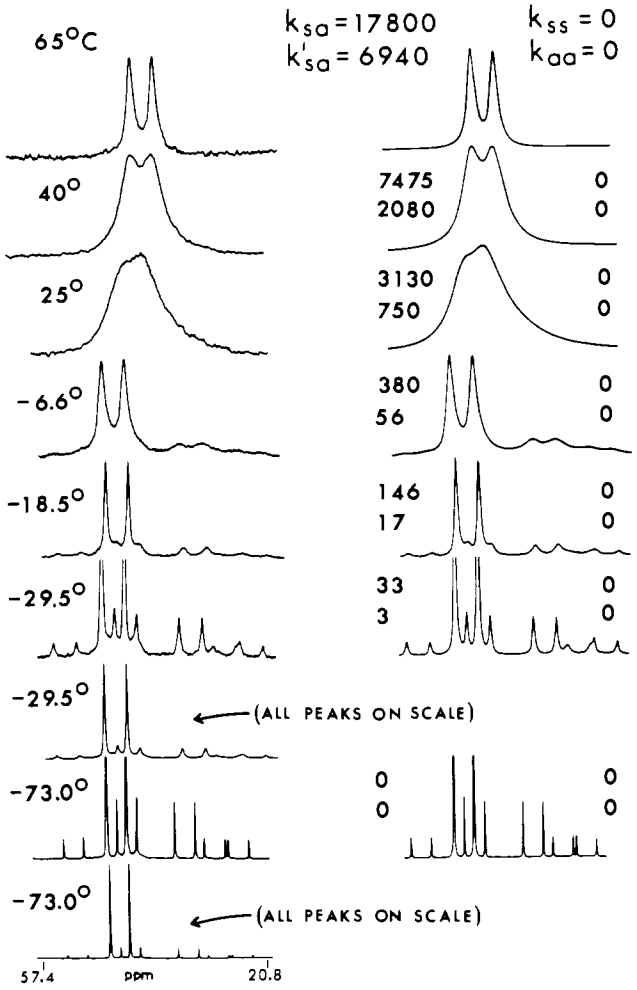

Figure 1. Experimental $^{31}P\{^1H\}$ pulsed FT DNMR spectra (36.43 MHz) (left column) of **1** (0.18 M in 50:50 CD_2Cl_2/toluene, v/v) and theoretical spectra (right column). k_{sa} = first-order rate constant (s^{-1}) for conversion of the minor syn rotamer (D_2X spectrum) to one anti (ACX or CAX); k'_{sa} is for the major syn rotamer (B_2X) to one anti; k_{ss} is for both the forward and reverse direct syn to syn processes; k_{aa} is for the direct anti to anti processes (ACX to CAX). See eq 1 for a definition of all the various rate constants. At -29.5 and -73.0 °C, the respective upper spectra are recorded with the B_2X doublet vertically off scale.

ulation 0.03), and the AC portion of an ACX spin system with one chemical shift at δ 46.48 ($^2J_{PP}$ = 315.0 Hz, $^1J_{RhP}$ = 118.0 Hz) and the other chemical shift at δ 30.56 ($^2J_{PP}$ = 315.0 Hz, $^1J_{RhP}$ = 120.0 Hz) with a relative population of 0.24. An analysis of this spectrum at -73 °C is shown in Figure 2, and a compilation of all NMR parameters is presented in Table I.

Such DNMR behavior is clearly consistent with slowing conformational exchange in **1** and the presence of phosphorus atoms rendered nonequivalent by virtue of their presence in different conformations. The B_2X and D_2X subspectra observed at -73 °C (Figure 2) must be due to two different geometries which respectively have two magnetically equivalent phosphorus atoms. However, the ACX spectrum reflects a molecular geometry in which the two phosphorus atoms are magnetically and stereochemically nonequivalent. Since ligand dissociation is not a factor over the temperature range of interest in this study (Figure 1), the most reasonable rate process which would account for the DNMR behavior of **1** is rotation about the Rh–P bonds.

An examination of scale models and interatomic distance calculations for various conformers of **1** using the computer program COORD (time-sharing version)[14] indicate clearly that

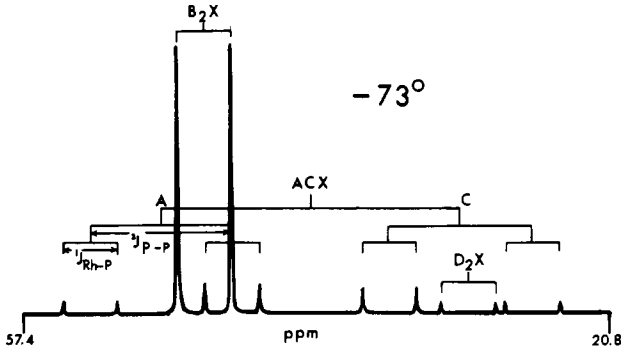

Figure 2. Analysis of the $^{31}P\{^1H\}$ NMR spectra of **1** at -73 °C.

the major steric repulsions for **1** involve a *tert*-butyl group on phosphorus eclipsing chlorine or carbon monoxide. Indeed, it is apparent that the preferred rotamer geometries for **1** involve a gauche orientation of the *tert*-butyl groups with respect to chlorine or carbon monoxide. A preferred gauche orientation for *tert*-butyl suggests an eclipsing of the chlorine and/or carbon monoxide by the *P*-methyl group. This rationale predicts four stable rotamers for **1** including two syn forms (**6** and **7**) and two equivalent anti forms (**8** and **9**) all of which are illustrated in eq 1. However, a perfect eclipsing

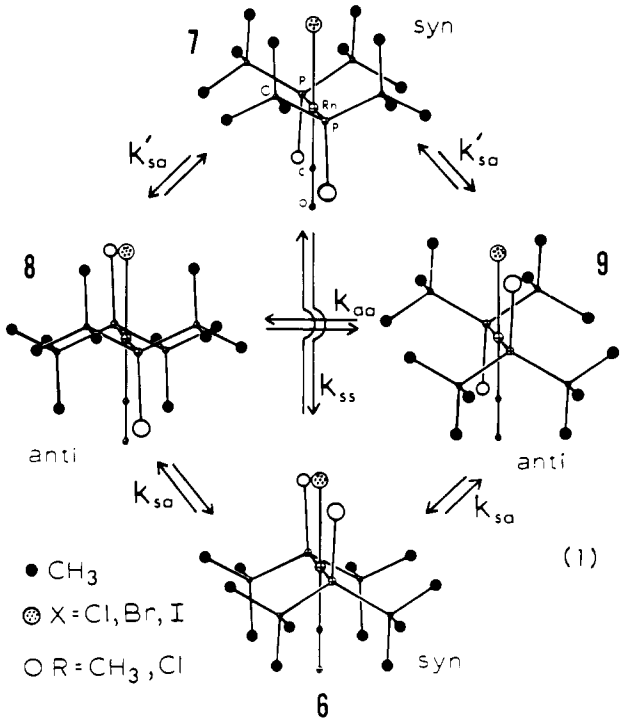

of the P–CH_3 and the Rh–Cl or Rh–CO bonds is probably not entirely reasonable on steric grounds. It is quite likely that such eclipsing would be relieved by a *slight* rotation about the Rh–P bond and/or a distortion of the Cl–Rh–CO bond angle away from 180°. Either or both of these events could lead to a very rapid "wagging" process (on the DNMR time scale) about the Rh–P bonds thus leading to time-averaged symmetries respectively equivalent to the symmetries of rotamers **6**–**9** (eq 1).

The two phosphorus atoms in the syn conformer **6** (eq 1) are *equivalent* and will have identical ^{31}P NMR chemical shifts. In the other syn form **7** (eq 1) the two phosphorus atoms are also equivalent but should have a ^{31}P NMR chemical shift different from **6** due to different local environments.

(14) Stevenson, P. E.; Merrill, J. E. Program No. 186, Quantum Chemistry Program Exchange; Indiana University: Bloomington, Ind., 1970.

Table I. ^{31}P DNMR Parameters, Rotamer Populations, and Activation Parameters for Rotation

compd	spin systems obsd at slow exchange	^{31}P NMR chem shifts, ppm[a]	$^1J_{RhP}$, Hz	$^2J_{PP}$, Hz	rel rotamer populations	rate process or spin exchange obsd	$\Delta H^{\ddagger}$, kcal/mol	$\Delta S^{\ddagger}$, eu	$\Delta G^{\ddagger}$, kcal/mol
1	B_2X	44.94	118.0		0.73 (−73 °C)	major syn to one anti	14.4 ± 0.3	3.1 ± 1.3	13.4 ± 0.1 (−7 °C)
	D_2X	28.97	120.0		0.03	one anti to minor syn	12.9 ± 0.4	−0.4 ± 1.5	13.0 ± 0.1 (−7 °C)
	ACX and CAX	46.48, 30.56	118.0, 120.0	315.0, 315.0	0.24				
2	A_2X	59.95	139.0		0.78 (−69 °C)	major syn to one anti	10.3 ± 0.7	−9.7 ± 2.8	12.7 ± 0.1 (−20 °C)
	B_2X	59.14	139.2		0.02	minor syn to one anti	10.3 ± 0.7	−9.7 ± 2.8	12.7 ± 0.1 (−20 °C)
	CDX and DCX	55.47, 46.01	142.4, 129.3	391.0, 391.0	0.20				
3	A_2X	60.71	140.0		0.03 (−52 °C)	major syn to one anti	14.7 ± 0.4	3.4 ± 1.3	13.8 ± 0.1 (−7 °C)
	B_2X	60.02	140.0		0.90	one anti to minor syn	13.2 ± 0.3	1.9 ± 0.4	12.7 ± 0.1 (−7 °C)
	CDX and DCX	53.46, 49.32	137.0, 137.0	390.0, 390.0	0.07				
4	A_2X	56.79	140.0		0.72 (−37 °C)	major syn to one anti	12.4 ± 0.4	−5.7 ± 1.4	13.9 ± 0.1 (0 °C)
	B_2X	56.46	140.0		0.02	minor syn to one anti	12.4 ± 0.4	−5.7 ± 1.4	13.9 ± 0.1 (0 °C)
	CDX and DCX	50.07, 48.44	134.0, 134.0	400.0, 400.0	0.26				
5	E_2X	53.23	120.0		0.30 (−117 °C)	ACX to BDX	8.3 ± 0.3	−1.1 ± 0.5	8.5 ± 0.1 (−73 °C)
	ACX and CAX	68.02, 54.16	117.0, 118.0	296.0, 296.0	0.24	BDX to DBX	8.7 ± 0.3	−3.9 ± 0.8	9.5 ± 0.1 (−73 °C)
	BDX and DBX	66.72, 54.08	117.0, 118.0	297.0, 297.0	0.46	BDX to E_2X	8.3 ± 0.3	−5.1 ± 1.0	9.4 ± 0.1 (−73 °C)

[a] Reference: external 85% H_3PO_4.

For each of the anti conformers **8** and **9** (eq 1), the two phosphorus atoms should be nonequivalent and give the observed AC portion of the ACX spectrum. In addition, the larger cone angle[7] for chlorine (102°) as compared to that of carbon monoxide (95°) would suggest that **7** is more stable than **6**. Thus, the large B_2X spectrum may be assigned to **7** (eq 1) and the much smaller D_2X spectrum to **6**. The ACX spectrum for **1** (Figure 2) is assigned to the two equivalent anti rotamers of **1** ((**8** and **9**) (eq 1)). These rotamer assignments are consistent with X-ray crystallographic data and $^{31}P\{^1H\}$ NMR spectra for some closely related rhodium and iridium complexes which have been studied by Shaw and co-workers.[12]

A complete $^{31}P\{^1H\}$ NMR line-shape simulation for **1** at −73 °C allows measurements of the relative concentrations of the various rotamers and, thus, free energy differences ($\Delta G°$) between rotamers. These values are complied in Table II for complexes **1**–**4**. The $\Delta G°$ values in Table II have not been adjusted for the statistical preference of two for the anti forms.

The conformational analysis for **1** described above implies the presence of *four* NMR detectable conformers, i.e., two different syn forms and two equivalent anti forms (eq 1). The fact that the two phosphorus atoms are nonequivalent in each anti form and exchange environments as a result of a direct anti to anti interconversion (e.g., **8** to **9** in eq 1) says that the $^{31}P\{^1H\}$ DNMR spectrum of **1** should be sensitive to this process as well as the other syn to anti and syn to syn processes in eq 1. Thus, eq 1 outlines multiple possibilities for conformational exchange pathways in **1**.

The kinetic model which gave the best fits of theoretical to experimental spectra (Figure 1) incorporated *no direct exchange* between syn forms and no direct exchange between anti forms. In generating the theoretical DNMR spectra, the rate constants corresponding to all direct syn to syn (e.g., **6** to **7** in eq 1) or anti to anti (e.g., **8** to **9**) processes were set at zero and exchange was allowed to occur in a stepwise fashion around the periphery of eq 1. The excellent fits with use of this model at various temperatures are illustrated in the right-hand column of Figure 1. In addition, systematic variations with temperature in relative conformer populations were introduced into the line-shape calculations. Relative conformer populations in the region of severe exchange broadening were determined from an extrapolation of data obtained from more sharply defined spectra at lower temperatures.

Table II. Free Energy Differences between Rotamers in the Complexes $[(t\text{-}C_4H_9)_2PR]_2Rh(CO)X$

	$\Delta G°$, kcal/mol (T, °C)[a]
1: R = CH_3; X = Cl	
syn (7 (eq 1))	most stable (−73 °C)
syn (6)	+1.3 ± 0.2
anti (8, 9)	+0.4 ± 0.1
2: R = X = Cl	
syn (7 (eq 1))	most stable (−69 °C)
syn (6)	+1.5 ± 0.2
anti (8, 9)	+0.6 ± 0.1
3: R = Cl; X = Br	
syn (7 (eq 1))	most stable (−52 °C)
syn (6)	+1.5 ± 0.2
anti (8, 9)	+1.1 ± 0.2
4: R = Cl; X = I	
syn (7 (eq 1))	most stable (−37 °C)
syn (6)	+1.7 ± 0.2
anti (8, 9)	+0.5 ± 0.1

[a] $\Delta G°$ values are not corrected for a statistical preference of 2 for the anti forms.

Other dynamical models which incorporated significant rates for the direct syn to syn and direct anti to anti processes gave clearly unacceptable fits to the experimental spectra. Even small values of k_{ss} and k_{aa} (see eq 1) caused a more rapid broadening of the A, C, and D resonances than observed experimentally. Accurate simulations of the experimental spectra are shown in the left-hand column of Figure 3. As examples of poor fits, a series of spectra incorporating various nonzero values of k_{ss} and k_{aa} are shown in the right-hand column of Figure 3. For the two spectra in which k_{sa} = 33, values of k_{ss} and k_{aa} as small as 1.0 cause an unacceptable and premature broadening of the A, C, and D resonances (e.g., see the peaks below the numeral one in Figure 3). At k_{sa} = 146 and k_{ss} and k_{aa} = 7, the ratios of the peak heights of the collapsed ACX signals to the B_2X signal are unacceptable. At higher rate constants (e.g., k_{sa} = 3130), significant nonzero values of k_{ss} and k_{aa} lead to an unacceptable skewing of the exchange-broadened resonance.

Thus, it is apparent from the line-shape analyses that the preferred itinerary for conformational exchange in **1** involves

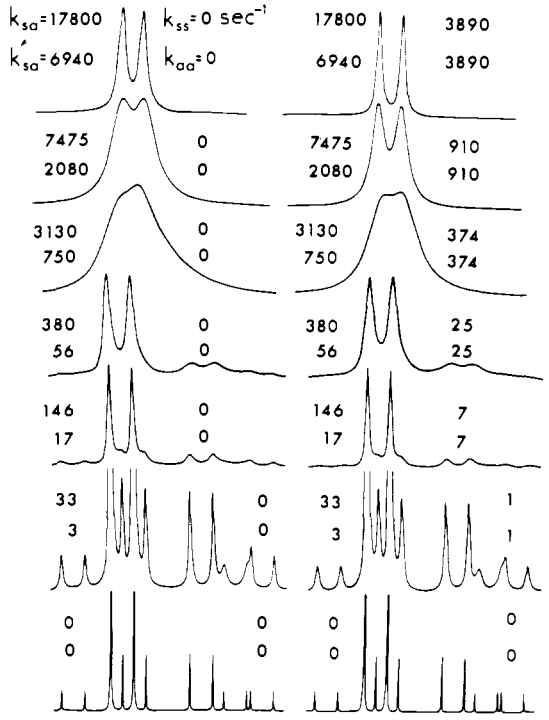

Figure 3. Comparison between the $^{31}P\{^1H\}$ DNMR spectra of **1** using an accurate simulation model (left column) (also see Figure 1) and a model which allows some direct syn to syn and some direct anti to anti equilibrations (right column). k_{sa}, k'_{sa}, and k_{aa} are defined in the caption to Figure 1 and also in eq 1. k_{ss} in this figure refers to the major syn to minor syn process.

stepwise conversions of **7** to **8**, **8** to **6**, **6** to **9**, **9** to **7**, etc., with no direct interconversions from **6** to **7** or **8** to **9** (eq 1). This stepwise exchange model is most consistent with simple internal rotation about the Rh–P bonds. Thus, it appears that conformational equilibration in **1** proceeds via stepwise rotations of one phosphine at a time with no simultaneous or concerted rotations of both phosphines. If simultaneous rotations of both phosphines occurred at a significant rate, the values of k_{ss} and k_{aa} (eq 1) required to fit the experimental spectra would of course be greater than zero, and they are not. This is satisfying intuitively because X-ray crystallographic studies of related complexes[12] indicate a negligible interaction between *tert*-butyl groups on different phosphines, and one would expect no cooperative effects on the rotation of phosphine ligands.

A consideration of models suggests that the maxima on the energy surface for conformational equilibration of **1** (eq 1) correspond to those geometries in which *tert*-butyl eclipses chlorine or carbon monoxide. Conversion of **7** to **8** (eq 1) involves initially one *tert*-butyl/chlorine eclipsing and then another *tert*-butyl/carbonyl eclipsing in the course of the conversion. From a statistical point of view, the preferred peripheral route for exchange is intuitively satisfying because the direct anti to anti and direct syn to syn conversions each require a series of four separate *tert*-butyl/ligand eclipsings. Although accurate DNMR line-shape simulations (Figure 1) incorporate no direct syn to syn or anti to anti processes, this does not necessarily mean that they do not occur. However, if they do occur, they occur at rates so much slower than other processes that they have no effect on the shape of the exchange-broadened DNMR spectra.

The activation parameters for conversion of the major syn rotamer of **1** to one anti form are $\Delta H^\ddagger$ = 14.4 ± 0.3 kcal/mol, $\Delta S^\ddagger$ = 3.1 ± 1.3 eu, and $\Delta G^\ddagger$ = 13.4 ± 0.1 kcal/mol at −7 °C and for conversion of one anti form to the minor syn rotamer $\Delta H^\ddagger$ = 12.9 ± 0.4 kcal/mol, $\Delta S^\ddagger$ = −0.4 ± 1.5 eu, and $\Delta G^\ddagger$ = 13.0 ± 0.1 kcal/mol at −7 °C. Activation parameters, rotamer populations, and various NMR parameters for **1** and the other complexes of interest in this report are compiled in Table I. A proposed free energy profile for conversion of **7** to **8** to **6** in eq 1 is presented in Scheme I. Those geometries in which the P–CH_3 group is in a plane perpendicular to the coordination plane are postulated as unstable intermediates.

Scheme I. Proposed Free Energy Profile for Rotation about the Rh–P Bonds in Complex **1**[a]

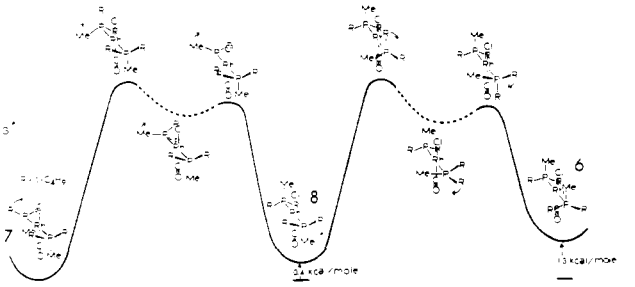

[a] The numbers **6–8** referring to different rotamers are the same numbers as those employed in eq 1. It is *assumed* that a *t*-C_4H_9/Cl eclipsing is of higher energy than a *t*-C_4H_9/CO eclipsing.

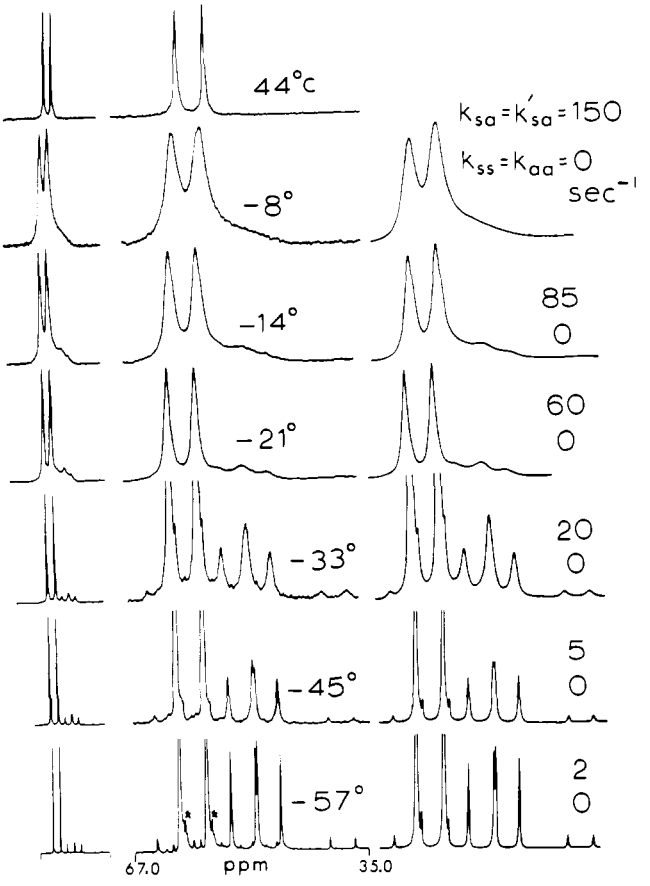

Figure 4. Experimental and theoretical $^{31}P\{^1H\}$ DNMR spectra (36.43 MHz) of **2** (2 M in 50:50 CD_2Cl_2/toluene). The far left column illustrates the experimental spectra with a compressed ppm scale and all vertical intensities on scale. The middle column of spectra illustrates the experimental spectra with an expanded ppm scale and the vertical intensity of the A_2X spectrum off scale at −33, −45, and −57 °C. The right-hand column illustrates theoretical spectra of **2** for which k_{sa} is the first-order rate constant (s^{-1}) for conversion of the minor syn rotamer (B_2X) to one anti (CDX or DCX); k'_{sa} is for the major syn rotamer (A_2X) to one anti; k_{ss} is for the direct minor syn to major syn process; k_{aa} is for the direct anti to anti process (CDX to DCX).

***trans*-Rh[P(*t*-C_4H_9)$_2$Cl]$_2$(CO)Cl (2).** The $^{31}P\{^1H\}$ DNMR spectrum of **2** (2 M in 50:50 CD_2Cl_2/toluene) at 44 °C shows a broadened doublet (δ 57.42, $^1J_{RhP}$ = 146 Hz, Figure 4). This

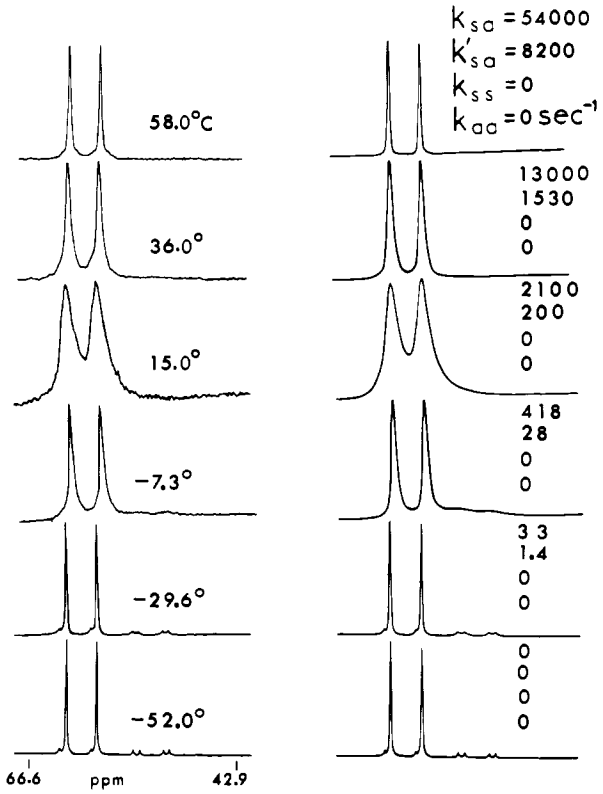

Figure 5. Experimental $^{31}P\{^1H\}$ DNMR spectra (36.43 MHz) (left column) of **3** (0.11 M in toluene-d_8) and theoretical spectra (right column). k_{sa} is for the minor syn (A_2X) to one anti (CDX or DCX) process; k'_{sa} is for the major syn (B_2X) to anti; k_{ss} and k_{aa} refer to the direct minor syn to major syn and direct anti to anti processes, respectively.

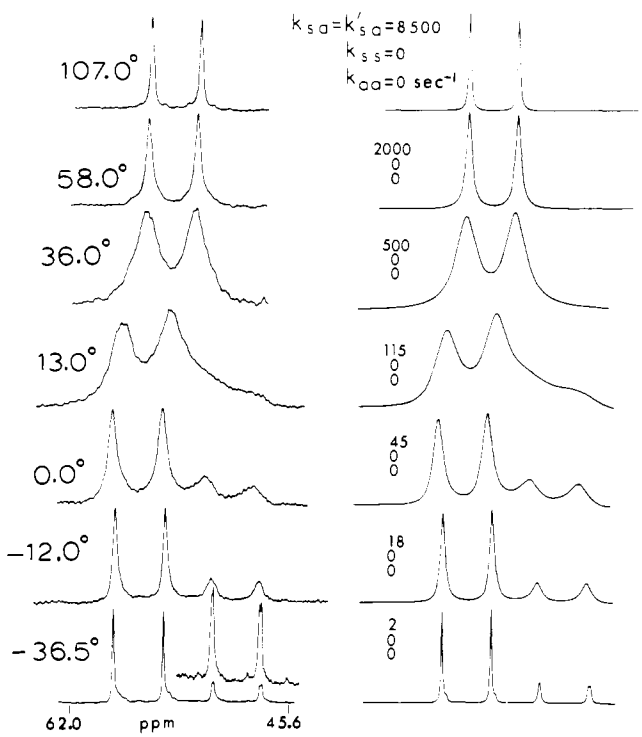

Figure 6. Experimental $^{31}P\{^1H\}$ DNMR spectra (36.43 MHz) (left column) of **4** (0.11 M in toluene-d_8) and theoretical spectra (right column). k_{sa} and k'_{sa} are the first-order rate constants (s^{-1}), respectively, for conversion of the minor syn rotamer (B_2X) to one anti (CDX or DCX) and for conversion of the major syn (A_2X) to one anti; k_{ss} and k_{aa} refer to the direct minor syn to major syn and anti to anti processes, respectively.

spectrum of **2** at 44 °C is consistent with rapid Rh–P bond rotation. At temperatures below 44 °C, the spectrum undergoes asymmetric broadening and then sharpens into a series of well-defined resonances at −57 °C (Figure 4). At −57 °C, the slow-exchange spectrum of **2** consists of a dominant A_2X doublet (relative population 0.78), the CD portion of a CDX spectrum (relative population 0.20), and a minor B_2X doublet (relative population 0.02) located just upfield of the much larger A_2X doublet (see asterisks at −57 °C in Figure 4). Various chemical shifts and coupling constants are compiled in Table I. The spectrum of **2** at −57 °C is similar in many respects to that of **1** at −73 °C (Figures 1 and 2). The two different doublet signals for **2** can be assigned to conformers in which the two phosphorus atoms are equivalent and the CD portion of a CDX spectrum is attributable to two nonequivalent phosphorus atoms in another type of conformer.

One would predict conformational preferences for **2** which are similar to those of **1**, i.e., **6**, **7**, **8**, and its equivalent anti form **9** ((X = R = Cl) (eq 1)). Indeed, the population distribution among the four rotamers of **2** is very similar to that in **1** (Tables I and II). Thus, the CDX spectrum for **2** may be assigned to the two equivalent anti forms **8** and **9** ((X = R = Cl) (eq 1)) and the doublet resonances to syn rotamers **6** and **7**. The relative energies of the two syn forms of **2** may be assigned with use of cone angle arguments analogous to those for **1** discussed above. Thus, for complex **2**, conformer **7** is predicted to be more stable than **6** (see Table II).

In simulating the exchange-broadened spectra of **2**, the dynamical model which gives the best spectral fits incorporates *no direct exchange* between equivalent anti forms or between the two different syn forms; i.e., the preferred pathway in eq 1 is a stepwise conversion of **7** to **8**, **8** to **6**, **6** to **9**, etc., which is completely analogous to complex **1** and consistent with simple internal rotation about the Rh–P bonds. Pertinent NMR, conformational, and activation parameters for **2** are compiled in Tables I and II.

***trans*-Rh[P(*t*-C_4H_9)$_2$Cl]$_2$(CO)Br (3).** The $^{31}P\{^1H\}$ DNMR spectrum of **3** (0.11 M in toluene-d_8) at 58 °C also shows a doublet at δ 58.93 ($^1J_{RhP}$ = 137 Hz) consistent with rapid equilibration on the DNMR time scale (Figure 5). The slow-exchange spectrum at −52 °C is composed of a small A_2X doublet (relative population 0.03), a major B_2X doublet (relative population 0.90), and two closely spaced *apparent* doublets upfield from the B_2X signals (Figure 5). In light of the line-shape analyses for **1** and **2**, these small upfield signals are best rationalized as the inner components of the CD portion of a minor CDX spectrum for which the outer lines are too small to be detected. The intensities of the outer lines of the CD part of the CDX subspectrum will be weak due to a small rotamer population and a small ratio of the CD chemical shift difference to the $^2J_{PP}$ value. With assumption of the same $^2J_{PP}$ value for **3** as that measured for the CDX subspectrum of **2** (391 Hz), the ^{31}P chemical shifts of the C and D resonances of **3** are computed to be δ 53.46 and 49.32 with both $^1J_{RhP}$ values measured directly (137.0 Hz). The relative population of the CDX spin system is 0.07. By analogy with complexes **1** and **2**, the dominant B_2X doublet is assigned to the syn rotamer **7** ((X = Br and R = Cl) (eq 1)), the minor A_2X doublet to **6**, and the CDX subspectrum to the anti rotamers **8** and **9**. Again, the stepwise peripheral route for exchange (eq 1) gave an excellent fit of theoretical to experimental DNMR spectra (Figure 5). Pertinent NMR, conformational, activation, and free energy parameters are compiled in Tables I and II.

***trans*-Rh[P(*t*-C_4H_9)$_2$Cl]$_2$(CO)I (4).** The $^{31}P\{^1H\}$ DNMR behavior for **4** (0.11 M in toluene-d_8) in which iodine is bonded to rhodium is very similar to that of **3** (Figure 6). At slow exchange (−36.5 °C), the spectrum consists of an A_2X doublet (relative population 0.72), a B_2X doublet (relative population

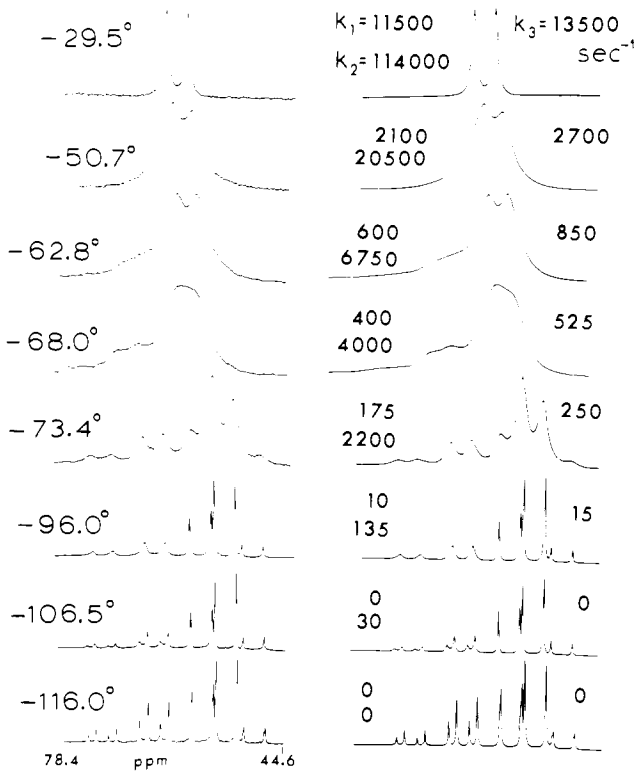

Figure 7. Experimental $^{31}P\{^1H\}$ DNMR spectra (36.43 MHz) (left column) of **5** (0.22 M in 80:20 CF_2Cl_2/CD_2Cl_2) and theoretical spectra (right column). The various rate constants listed are defined according to eq 2. Only the values of k_1,k_2,k_3, and the rate constants for each respective back-reaction were varied to fit the experimental spectra. The values k_4,k_5,k_6, and the rate constants for each respective back-reaction were kept at zero throughout.

0.02), and the CD portion of a CDX spin system (relative population 0.26). The outer lines of the C and D resonances are not observed due to a small chemical shift to coupling constant ratio. The C and D chemical shifts compiled in Table I were calculated with assumption of a $^2J_{PP}$ value of 400 Hz. Again, a dynamical model which incorporates no direct syn to syn or anti to anti interconversions gave the best fit of theoretical to experimental DNMR spectra for **4**, and pertinent activation parameters are compiled in Table I.

***trans*-Rh[P(*t*-C$_4$H$_9$)$_2$(C$_6$H$_5$)]$_2$(CO)Cl (5).** The $^{31}P\{^1H\}$ DNMR spectrum of **5** at slow exchange is more complicated than those for complexes **1–4**, revealing a change in rotamer preferences. The exchange-broadened spectra also reveal different dynamics for equilibration as compared to those for **1–4**. The spectra for **5** are illustrated in Figure 7. At room temperature, the $^{31}P\{^1H\}$ DNMR spectrum of **5** (0.22 M in CD_2Cl_2) consists of a sharp doublet centered at δ 60.1 ($^1J_{RhP}$ = 124 Hz). At lower temperatures in 80:20 CF_2Cl_2/CD_2Cl_2 as solvent (Figure 7), the spectrum of **5** undergoes a series of complex changes and is sharpened into a series of well-resolved resonances at −116 °C. A complete line-shape analysis of the spectrum at −116 °C reveals an E_2X doublet (X = ^{103}Rh; relative population 0.30), the AC portion of an ACX spectrum (relative population 0.24), and the BD portion of a BDX spectrum (relative population 0.46). Various chemical shifts and coupling constants are compiled in Table I. These various subspectra are identified in Figure 8. The conformational preferences in **5** are different from those for complexes **1–4** in that only one type of NMR detectable conformation for **5** has both phosphorus atoms equivalent and *two* other types have *nonequivalent* phosphorus atoms. In complexes **1–4**, it should be noted that only one type of rotamer, i.e., the anti form (eq 1), was observed to have nonequivalent phosphorus atoms.

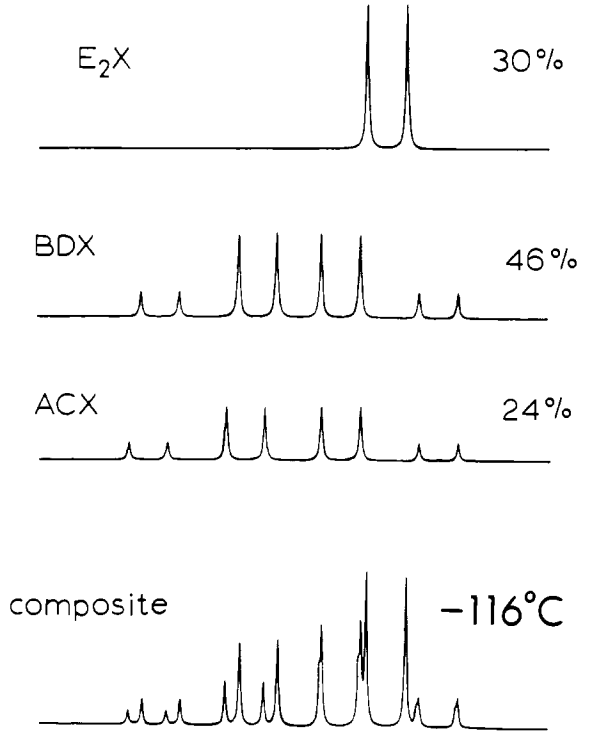

Figure 8. Decomposition of the $^{31}P\{^1H\}$ NMR spectrum of **5** into component subspectra at −116 °C. Each percentage reflects the area of each subspectrum as compared to the total area of the complete spectrum (see "composite" spectrum). Addition of the properly weighted E_2X, BDX, an ACX spectra produces the composite spectrum.

An examination of models and interatomic distance calculations for **5** analogous to those performed for **1** reveal that steric interactions between the *tert*-butyl groups, and the ligands on rhodium are optimized when phenyl eclipses a ligand (e.g., see **10** in eq 2). This is similar to complex **1**. However,

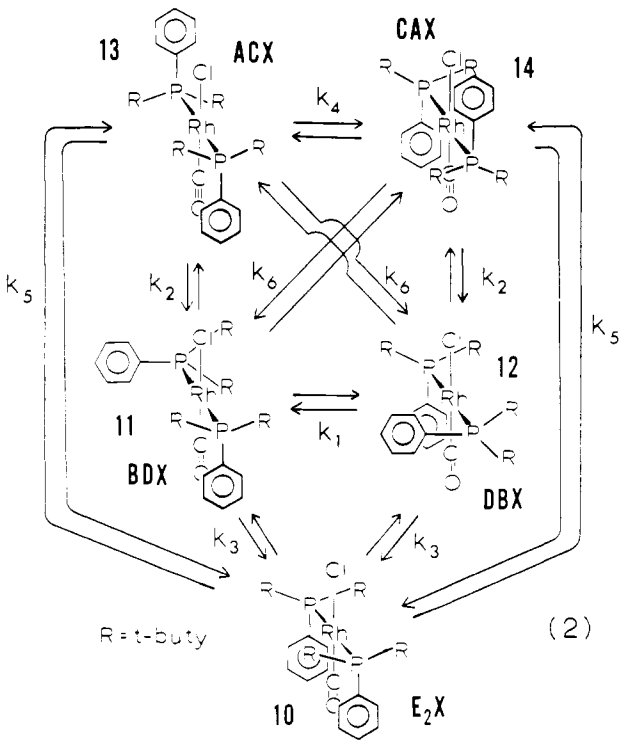

an examination of models indicates also that the phenyl groups in **10** cannot be coplanar with the coordination plane about rhodium and must be skewed about the phenyl–phosphorus

bond. Indeed, the extent of phenyl skewing is in turn restricted by a buttressing effect of the proximate *tert*-butyl groups on the same phosphine. The net result is that the phenyl-eclipsing carbonyl in rotamer **10** appears to experience a greater repulsion than the analogous eclipsed methyl in complex **1** (see **7** in eq 1). Such generally increased crowding associated with the phenyl groups in **5** could lead to detectable concentrations of rotamer types not observed in complexes **1–4**.

With use of cone angle arguments presented earlier, that syn conformation of **5** in which both phenyls approximately eclipse *chlorine* would be predicted to be less stable than **10** (eq 2) in which they eclipse carbon monoxide. Thus, the E_2X doublet identified in Figure 8 may be assigned to the syn form **10** in eq 2.

In light of the increased steric requirements of phenyl as compared to methyl, the anti forms **13** and **14** (eq 2) would appear to be likely stable rotamers. The carbonyl and chlorine ligands may optimize interactions with the eclipsed phenyl groups by bending away from phenyl. In **10**, it is not possible for carbonyl to relax by bending in the plane of coordination due to the mutual buttressing effect of the two eclipsed phenyl groups. However, relaxation could occur via a reduction of the Cl–Rh–CO bond angle below 180°. Conformations such as **13** and **14** also satisfy the requirement of having two *nonequivalent* phosphorus atoms as revealed in either the ACX or the BDX subspectrum (Figure 8). Thus, the presence of anti rotamers **13** and **14** (eq 2) account for either the ACX or the BDX subspectrum but not both. One must postulate another conformation in which both phosphorus atoms are nonequivalent.

In light of the substantial steric size of phenyl, a conformation in which phenyl is out of the coordination plane of rhodium seems reasonable, e.g., **11** or **12** (eq 2). In **11** or **12**, the two phosphorus atoms are indeed nonequivalent. While steric repulsions involving the *tert*-butyl groups on the phosphine having phenyl out of the coordination plane have increased relative to **10** or **13** (eq 2), repulsions involving the phenyl group have indeed been relieved. The geometries **11** and **12** may be able to optimize the one phenyl eclipsing via bending away of the carbon monoxide ligand.

Assignment of rotamers to the ACX and BDX spin systems cannot be done unequivocally. However, tentative assignments are based on the following rationale. The chemical shift difference between the A and C phosphorus atoms of the ACX spectrum is 13.86 ppm which is 1.22 ppm greater than that between the B and D phosphorus atoms (12.64 ppm) of the BDX spectrum. This might suggest that the rotamer corresponding to the ACX spectrum possesses two phosphorus atoms in environments more different than those for the rotamer giving the BDX spin system. Intuitively, the ACX spectrum may then be assigned to the anti rotamers (**13** and **14**) in which the two phenyl groups are eclipsing quite different ligands. The BDX spectrum is assigned to **11** and **12**. These assignments albeit somewhat arbitrary are internally consistent with the stereodynamical picture of **5** derived from DNMR line-shape analyses described below. Thus, it is apparent that rotamers **11** and **12** are more stable than **10** ($\Delta G^\circ = -0.13 \pm 0.10$ kcal/mol at −116 °C) and also more stable than **13** and **14** ($\Delta G^\circ = -0.20 \pm 0.10$ kcal/mol at −116 °C).

On the basis of the DNMR and rotamer assignments discussed above, a general exchange pathway for **5** may be constructed and is illustrated in eq 2. The spin system assigned to each rotamer of **5** is written beside the appropriate rotamer in eq 2. Exchange could occur among *five spin systems*: ACX, CAX, BDX, DBX, and E_2X.

So that the best fits of theoretical to experimental DNMR spectra for **5** (Figure 7) could be obtained, *no direct exchange* was allowed between the ACX and CAX spin systems, between the ACX and DBX spin systems, between the CAX and BDX spin systems, between the ACX and E_2X spin systems, or between the CAX and E_2X spin systems. The processes for which nonzero rate constants gave excellent fits include the ACX to BDX, CAX to DBX, BDX to DBX, BDX to E_2X, and DBX to E_2X equilibrations (eq 2). Of the processes which the total line-shape analyses indicated could occur, one type had an activation energy clearly lower than the others. The lowest barrier processes involve excange between the ACX and BDX spin systems and between the CAX and DBX systems. The phenomenon is best illustrated in the spectra between −96 and −116 °C in Figure 7. The E_2X doublet remains sharp but the ACX and BDX spectra are clearly subject to exchange broadening. It is clear from the line-shape analysis that any equilibrations involving the E_2X spin system and the BDX to DBX processes have barriers higher than the ACX to BDX or CAX to DBX equilibrations. At −96 °C, the rate constant for the ACX to BDX process is 135 s^{-1} while those for the BDX to DBX and E_2X to BDX processes are 10 and 15 s^{-1}, respectively. Pertinent activation and NMR parameters for **5** are compiled in Table I.

For a demonstration of the lack of validity of a dynamical model for **5** which involves direct exchange among all rotamers (i.e., a random exchange process), a series of theoretical DNMR spectra were generated in which k_1–k_6 values in eq 2 were all set equal. All respective back-reaction rate constants were given values reflecting each individual equilibrium distribution. The right-hand column of Figure 9 illustrates a number of those spectra which should be compared to those in the left-hand column which correspond to accurate fits to the experimental spectra. It is clear that a random exchange model does not pertain.

It is interesting to note that the lowest barrier rate processes involving Rh–P bond rotation in **5** (i.e., the ACX to BDX or CAX to DBX equilibrations) apparently involve a simple 90° rotation of one phosphine during which one *tert*-butyl group eclipses *carbonyl* in the transition state for rotation ($\Delta G^\ddagger$ = 8.5 kcal/mol at −68 °C). The E_2X to BDX process also involves a simple 90° rotation, but *tert*-butyl eclipses *chlorine* in the process and the barrier is higher ($\Delta G^\ddagger$ = 9.3 kcal/mol at −68 °C). These observations are consistent with a larger cone angle for chlorine (102°) as compared to carbonyl (95°) and a greater repulsion for *tert*-butyl eclipsing chlorine.[7] The BDX to DBX process involves two separate 90° rotations and two separate *tert*-butyl/chlorine eclipsings ($\Delta G^\ddagger$ = 9.4 kcal/mol at −68 °C). All other rate processes involving Rh–P rotation are apparently slower on the ^{31}P DNMR time scale and do not contribute significantly to the line shape.

One final comment needs to be made regarding complex **5**. While we have assigned the ACX and BDX subspectra to anti and skewed conformations resulting from restricted Rh–P bond rotation (i.e., **11–14**), the ACX and BDX subspectra could also result from anti conformers in which the phenyl groups are twisted in the same sense relative to one another in one anti form and in different senses relative to one another in another anti conformer. These species would, of course, be diastereomeric, and four different ^{31}P NMR signals could in principle be observed. Although such an occurrence is possible, it would require an unusually high barrier for the phenyl twisting process, and we consider it to be an unlikely source for the DNMR behavior for **5**.

A perusal of the activation parameters for rhodium–phosphorus bond rotation for complexes **1–4** (Table I) reveals no substantial differences in barriers to rotation in spite of a significant variation in substituents. However, in complex **5**, the barriers to Rh–P bond rotation are consistently lower than complexes **1–4** (Table I) in spite of an effectively larger steric bulk for phenyl as compared to methyl and halogen. Thus,

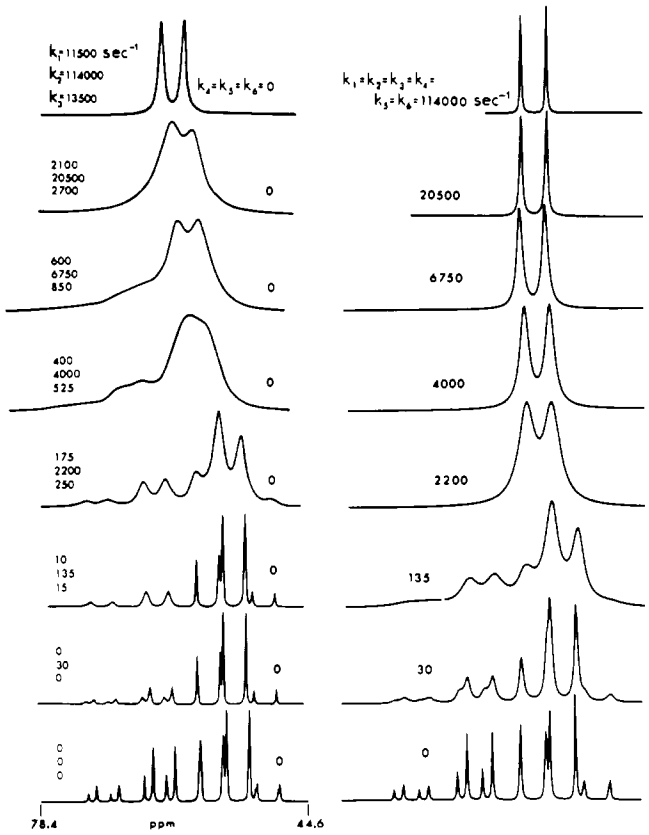

Figure 9. Best fit of theoretical $^{31}P\{^1H\}$ DNMR spectra of **5** to the experimental (left column) (also see Figure 7). k_1–k_6 defined in eq 2 all set equal with all back-reaction rate constants adjusted to reflect equilibrium populations (right column).

the lower barriers in **5** might reflect increased crowding in the ground state (as compared to **1**–**4**) leading to a compression of ground-state and rotational transition-state energy differences and thus lower barriers.[7] Increased crowding in **5** could also lead to an elongated Rh–P bond and have consequences on the rate of rotation. It is also possible that different electron-donor properties for $(t\text{-}C_4H_9)_2P(C_6H_5)$ as compared to the phosphines in complexes **1**–**4** lead to an alteration of the stereodynamics of the Rh–P bond.

Experimental Section

The 36.43-MHz $^{31}P\{^1H\}$ FT DNMR spectra were recorded with use of a Bruker HFX-90/Digilab FTS/NMR-3 spectrometer. All solvents used for synthesis and for DNMR samples were thoroughly degassed.

Theoretical DNMR spectra were calculated with use of DEC PDP-10 computer and plotted with use of a Calcomp plotter.

***trans*-Rh(Cl)(CO)[P(t-C_4H_9)$_2$$CH_3$]$_2$ (1).** Di-*tert*-butylmethylphosphine[15] (0.000 21 mol) was added to a solution of bis(μ-chloro)-tetracarbonyldirhodium (0.000 05 mol) in degassed benzene (30 mL) under a nitrogen atmosphere. The deep red solution of the rhodium(I) dimer turned bright yellow immediately, and a gas (CO) was evolved. The solution was allowed to stir at room temperature for 3 h and then concentrated to about 15 mL under vacuum. Addition of cold methanol caused the product to separate from solution as bright yellow sparkling crystals. These crystals were recrystallized from benzene/methanol three times and dried under vacuum.

Anal. Calcd for $C_{19}H_{42}ClOP_2Rh$: C, 46.88; H, 8.70; Cl, 7.28. Found: *C*, 46.79; H, 8.43; Cl, 6.93.

***trans*-Rh(Cl)(CO)[P(t-C_4H_9)$_2$Cl]$_2$ (2).** This complex was prepared as above using di-tert-butylchlorophosphine (Strem Chemicals, Inc.).

Anal. Calcd for $C_{17}H_{36}Cl_3OP_2Rh$: C, 38.70; H, 6.88; Cl, 20.16. Found: C, 38.58; H, 6.74; Cl, 20.24.

***trans*-Rh(Br)(CO)[P(t-C_4H_9)$_2$Cl]$_2$ (3).** This complex was prepared from complex **2** by six separate exchanges with use of a stirred 6 molar excess of lithium bromide in methanol at reflux for 3 h. At the end of each exchange, the methanol solution was cooled (0 °C) whereupon the rhodium complex precipitated. The solid complex was then washed with water and methanol several times and subjected to a subsequent treatment with lithium bromide in refluxing methanol. After the last exchange, the precipitate was washed with water and methanol and recrystallized three times from methanol/benzene.

Anal. Calcd for $C_{17}H_{36}Cl_2BrOP_2Rh$: C, 35.69; H, 6.34; Br, 13.97; Cl, 12.39. Found: C, 35.64; H, 6.15; Br, 13.68; Cl 12.22.

***trans*-Rh(I)(CO)[P(t-C_4H_9)$_2$Cl]$_2$ (4).** This complex was prepared from complex **2** by six separate exchanges with use of a stirred 6 molar excess of sodium iodide in refluxing methanol for 3 h as described for complex **3** above. Complex **4** was purified by three recrystallizations from methanol/benzene.

Anal. Calcd for $C_{17}H_{36}Cl_2IOP_2Rh$: C, 32.98; H, 5.86; I, 20.51; Cl, 11.45. Found: C, 33.04; H, 5.79; I, 20.31; Cl, 11.31.

***trans*-Rh(Cl)(CO)[P(t-C_4H_9)$_2$$C_6H_5$]$_2$ (5).** This complex was prepared according to the procedure for **1** above with use of di-*tert*-butylphenylphosphine.[16]

Anal. Calcd for $C_{29}H_{46}ClOP_2Rh$: C, 57.01; H, 7.59; Cl, 5.80. Found: C, 57.66; H, 7.21; Cl, 5.68.

Acknowledgment. We are grateful to the National Science Foundation (Grant Nos. MPS74-17544, CHE76-80356, and CHE77-06749) for support and to the Worcester Area Colleges Computation Center for donated computer time. We also acknowledge Dr. C. A. Tolman for many helpful comments as well as Mr. G. Watunya and Mr. R. D. Ballback for running many of the NMR spectra.

Registry No. **1**, 34365-67-8; **2**, 78246-82-9; **3**, 78199-31-2; **4**, 78199-32-3; **5**, 32628-32-3; di-μ-chloro-tetracarbonyldirhodium, 14523-22-9.

(15) Crofts, P. C.; Parker, D. M. *J. Chem. Soc. C* **1970**, 332.
(16) Mann, B. E.; Shaw, B. L.; Slade, R. M. *J. Chem. Soc. A* **1971**, 2976.